Overload Retardation Due to Plasticity-induced Crack Closure

N. A. FLECK and H. R. SHERCLIFF
Cambridge University Engineering Department, Trumpington Street, Cambridge CB2 1PZ, UK

ABSTRACT

Experiments are reported which show that plasticity-induced crack closure can account for crack growth retardation following an overload. The finite element method is used to provide evidence which supports the experimental observations of crack closure. Finally, a simple model is presented which predicts with limited success the retardation transient following an overload.

KEYWORDS

Fatigue crack closure; finite element method; variable amplitude loading; crack growth retardation.

EXPERIMENTAL WORK

Overloads were applied to 3 mm thick and 24 mm thick compact tension specimens made from a 25 mm thick plate of BS4360 50B steel. This steel has a composition (in wt %) of 0.14 C, 1.27 Mn, 0.41 Si, 0.017 P, 0.004 S, 0.073 Al, and has a yield stress σ_y of 352 MPa and an ultimate tensile stress σ_{uts} of 519 MPa. Specimens were stress relieved prior to testing.

Fatigue cracks were grown transverse to the roll direction at a constant stress intensity range ΔK and constant load ratio R ($= P_{min}/P_{max}$), by manually shedding the load with crack growth. The test frequency was 5 Hz. The crack length was monitored using a travelling microscope and the D.C. potential drop method. Crack closure was monitored using back face strain and crack mouth displacement gauges. An offset procedure and low-pass filters were used to improve accuracy of the closure measurements. Further information about the instrumentation used is given in Fleck (1982), Fleck (1984) and Fleck *et al.*(1983).

A single overload of range twice the baseline load range was applied and the baseline loading was then resumed. Results with details of loading conditions are presented in Fig.1. Crack growth rates inferred from the

closure measurements are included in Fig.1. From the observed effective stress intensity range ΔK_{eff} (= maximum stress intensity, K_{max}, minus crack opening stress intensity, K_{op}) crack growth rates are predicted using the constant amplitude correlation (Fleck, 1984):

$$\frac{da}{dN} = 1.07 \times 10^{-8} (\Delta K_{eff})^{2.95} \quad \text{mm/cycle} \qquad (1)$$

where ΔK_{eff} is in MPa$\sqrt{m}$.

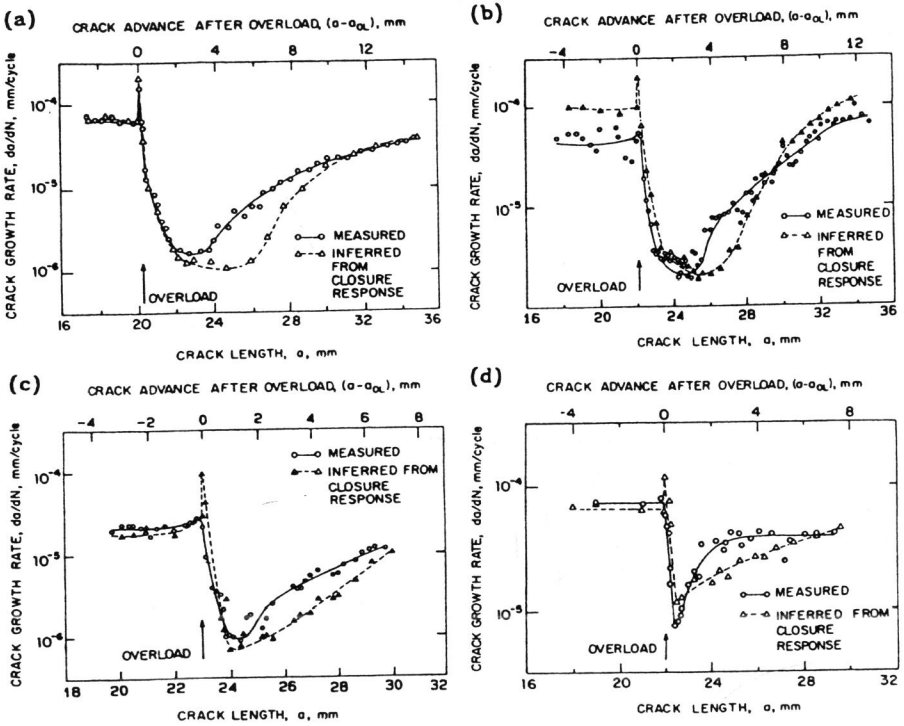

Fig. 1. Comparison of measured crack growth rates with values inferred from closure measurements. Arrow denotes the application of a single overload of range twice the baseline loading. Baseline loading conditions for 3 mm thick specimens (plane stress):
(a) ΔK = 25 MPa$\sqrt{m}$, R = 0.05
(b) ΔK = 25 MPa$\sqrt{m}$, R = 0.3
(c) ΔK = 20 MPa$\sqrt{m}$, R = 0.05
and for 24 mm thick specimen (plane strain):
(d) ΔK = 25 MPa$\sqrt{m}$, R = 0.05.

Consider first the results for the 3 mm thick specimens, Figs.1(a)-(c). These specimens are sufficiently thin for plane stress conditions to exist along the crack front. The crack remains sensibly straight along its front

during the test and the retardation transient predicted by the potential drop method and visual observations are similar. After application of an overload the crack growth rate and ΔK_{eff} decrease until a minimum is reached when the crack has grown a distance of about one quarter of the overload plastic zone size. Thereafter the crack growth rate and ΔK_{eff} increases towards the steady state pre-overload values. There is good agreement between the measured and predicted growth rates except for the period when the crack growth rates are recovering from the minimum post-overload value towards the steady-state value. During this period measured crack growth rates are faster than the predicted values. It is thought that this discrepancy is due to discontinuous closure - after the crack has grown a distance into the overload plastic zone it shuts first at a location between the overload crack length and the current crack tip position. Cyclic displacements and associated "fatigue damage" are experienced by the crack tip at loads below the closure load. Then the measured crack growth rate is faster than that predicted by closure measurements. Direct evidence of discontinuous closure is given in Fig.2 for the 3 mm thick specimen which was subjected to baseline loading of ΔK = 25 MPa$\sqrt{m}$ and R = 0.3. The figure shows a montage of positive replicas of the crack profile, taken when the crack has grown 5.5 mm beyond the overload location. At $K = K_{mean} = (K_{max} + K_{min})/2$, the crack is open near its tip but closed near the overload location. When the load is reduced to $K = K_{min}$ the crack tip shuts and the crack is fully closed back to the overload location.

Now consider results for the 24 mm thick specimen, Fig.1(d). This specimen is sufficiently thick for plane strain conditions to prevail along most of the crack front. The crack growth response has been deduced from the potential drop method, since this technique is more suited to measure bulk response than surface visual measurements of crack length. It has been found previously that the back face strain gauge and crack mouth gauge provide accurate bulk measurements of crack closure (Fleck and Smith, 1982, Fleck *et al.*, 1983). It is deduced from Figs.1(a) and (d) that retardation is less pronounced under plane strain conditions than under plane stress conditions. It is thought that the discrepancy between predicted and measured crack growth rates in Fig.1(d) is again due to discontinuous closure. We conclude from these experiments that plasticity-induced crack closure is able to account for retardation following an overload in BS4360 50B steel, when the pre-overload growth rates are far above threshold.

FINITE ELEMENT CALCULATIONS

The effect of an overload on plasticity-induced crack closure following a tensile overload was modelled using the finite element method. Using a program developed by Newman (1976) and discussed elsewhere (Fleck, 1986, Fleck and Newman, 1988), crack growth was simulated in centre-cracked panels (CCP) and in bend specimens made from elastic-perfectly plastic material of yield strain 0.005 and Poisson's ratio υ = 0.3.

The finite element mesh consisted of 1967 two-dimensional constant strain triangular elements; near the crack tip the elements were arranged to form a series of squares and their diagonals in order to accommodate incompressible flow (Nagtegaal *et al.*, 1974). Fictitious springs were used to change the boundary conditions associated with crack growth, crack closure or crack opening. Fatigue crack growth was simulated by release of the crack tip

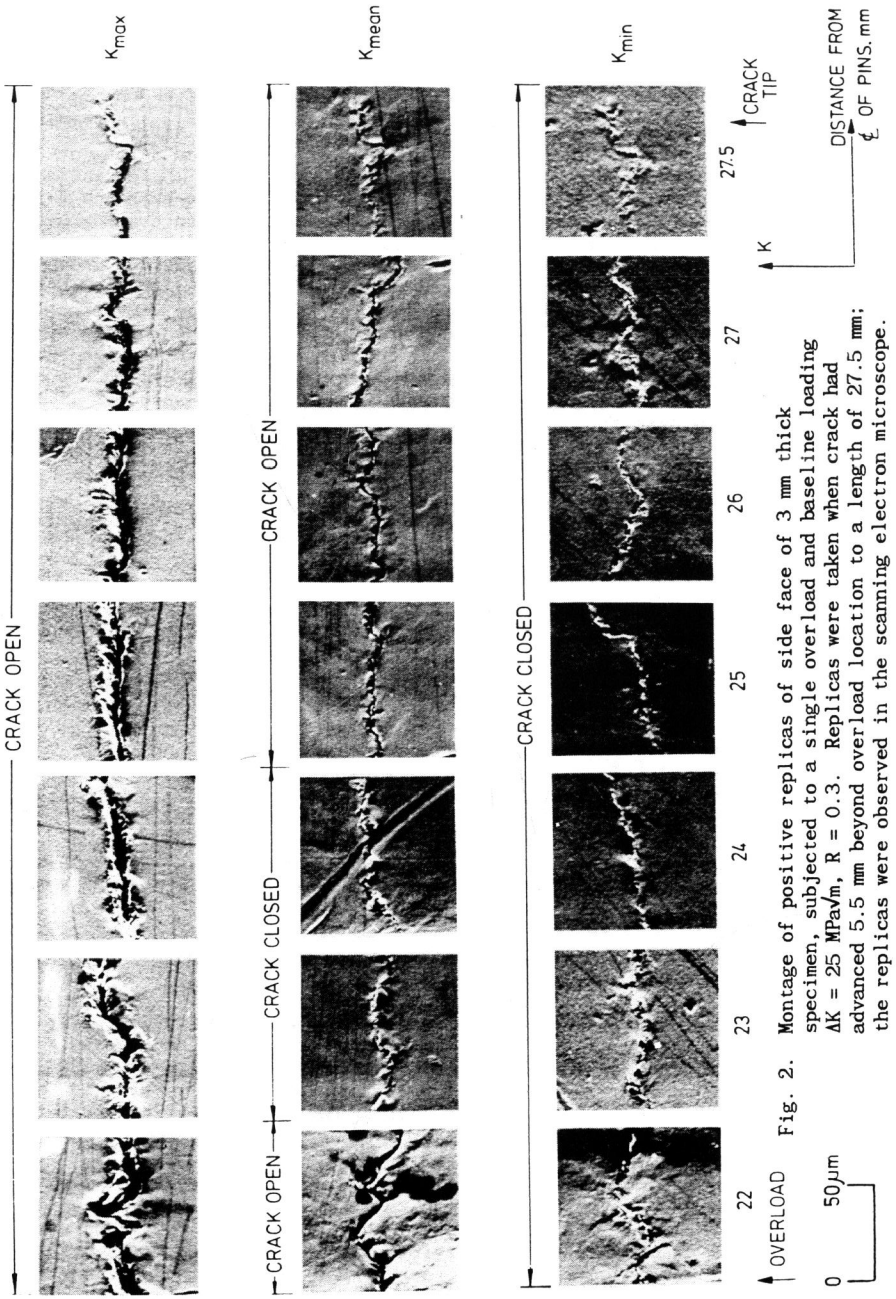

Fig. 2. Montage of positive replicas of side face of 3 mm thick specimen, subjected to a single overload and baseline loading ΔK = 25 MPa$\sqrt{m}$, R = 0.3. Replicas were taken when crack had advanced 5.5 mm beyond overload location to a length of 27.5 mm; the replicas were observed in the scanning electron microscope.

node at K_{max}, followed by a single loading cycle: $K_{max} \rightarrow K_{min} \rightarrow K_{max}$, and this process was then repeated. Typically, a crack was advanced by 6 small element sizes (each of size 0.00078125 w, where w is the width of the specimen) from an initial crack length a of 0.486719 w, under fatigue loading. An overload of range twice the baseline loading was applied with no crack growth, and then baseline loading was resumed for a crack growth increment of 30 element sizes. Both plane stress and plane strain conditions were considered: for the plane stress runs, the baseline $K_{max} = 0.11\ \sigma_y \sqrt{w}$ and $K_{min} = 0$, while for the plane strain runs, the baseline $K_{max} = 0.22\ \sigma_y \sqrt{w}$ and $K_{min} = 0$.

The overload plastic zone at $K = K_{ol}$ is shown in Fig.3(a) for plane stress, and in Fig.3(b) for plane strain. The overload plastic zone extends further ahead of the crack tip under plane stress conditions than under plane strain conditions. While specimen geometry has little influence upon plastic zone shape in plane stress, the zone is larger and extends further ahead of the crack for the CCP geometry than for the bend geometry under plane strain conditions. Larsson and Carlsson (1973) have shown that this variation in plastic zone shape with specimen geometry for plane strain is due to the different magnitudes of the "T-stress" near the crack tip in the two geometries. Specifically, the non-singular second term in the series expansion of the normal stress parallel to the crack plane differs from one geometry to the next, and has a strong influence on plastic zone size and shape.

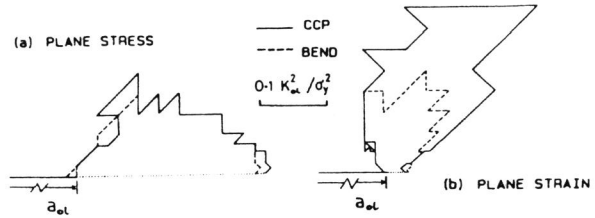

Fig. 3. Overload plastic zones predicted by finite element analysis for: (a) plane stress, and (b) plane strain.

A plot of the ratio of crack opening load to the maximum load of the fatigue cycle, P_{op}/P_{max}, is given in Fig.4 as a function of crack extension from the overload location, for both geometries and stress states. It is clear that the crack opening load is higher and persists over a larger crack growth increment for plane stress conditions than for plane strain. Under plane stress loading, specimen geometry has little influence on the closure transient, whereas under plane strain loading there is a stronger closure transient in the CCP geometry than in the bend geometry. This is consistent with the fact that the overload plastic zone is larger in the CCP geometry than in the bend geometry, under plane strain conditions.

Predicted closure transients are compared with the experimental results for the BS4360 50B steel in Fig.5. There is reasonable agreement for both the 3 mm and 24 mm thick specimens, supporting the hypothesis that retardation in these specimens is due to plasticity-induced crack closure.

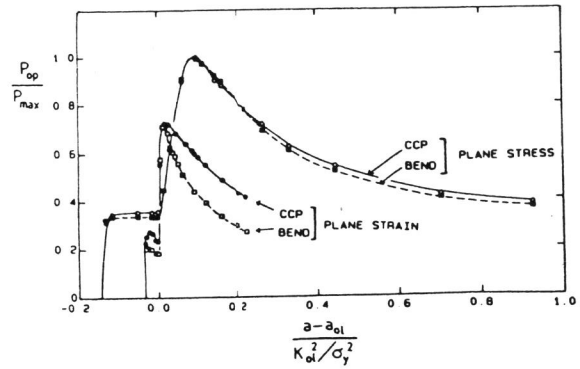

Fig. 4. Finite element prediction of crack opening response following an overload.

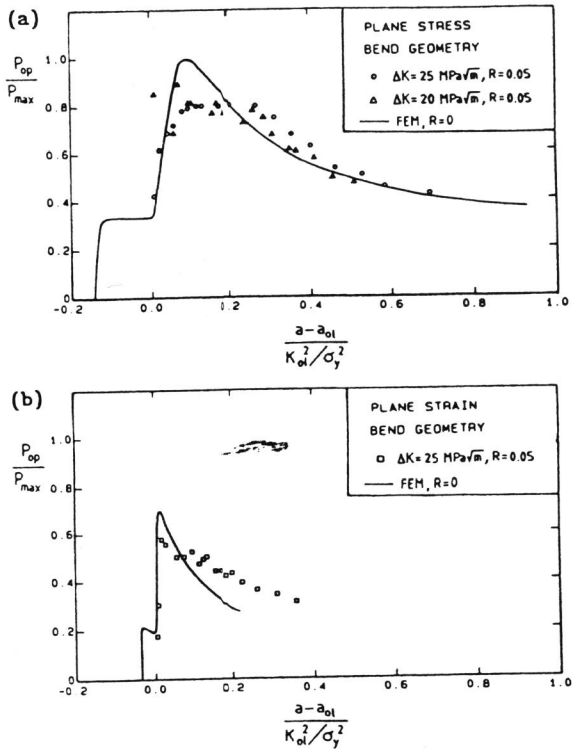

Fig. 5. Comparison of finite element prediction with measured crack opening response following an overload for: (a) plane stress, and (b) plane strain.

Crack opening profiles at K_{min} are shown in Fig.6 when the crack has advanced to near the boundary of the overload plastic zone. Consistently, the crack is open near its tip and shut near the overload location. This is the same phenomenon of discontinuous closure as was observed for both thicknesses of steel specimen.

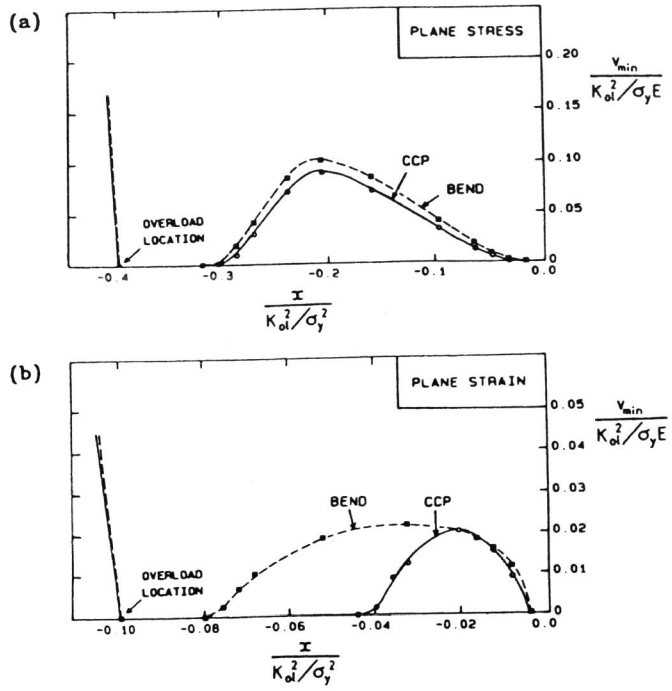

Fig. 6. Finite element prediction of crack opening profiles at K_{min} following an overload.

(a) Plane stress, crack has advanced 0.4 $(K_{ol}/\sigma_y)^2$ ahead of the overload location.

(b) Plane strain, crack has advanced 0.1 $(K_{ol}/\sigma_y)^2$ ahead of the overload location.

SIMPLE MODEL OF OVERLOAD RETARDATION

A simple model is now developed in order to predict retardation following an overload on the basis of plasticity-induced crack closure. From an assumed distribution of residual stress induced by the overload, a transient K_{op} versus crack extension Δa response is calculated and hence the retardation behaviour. In more detail, the model consists of the following steps:

1. Following Stouffer and Williams (1979), the crack tip stress

distribution found by Rice (1967) for mode III loading is used to estimate the stress component σ_{yy} normal to the cracking plane as a function of distance x ahead of the crack tip:

$$\sigma_{yy}\,\epsilon_{yy} = \frac{K^2}{\pi\,(1+n)\,E\,x} \qquad (2)$$

Here ϵ_{yy} is the local true strain component related to σ_{yy} via the constitutive law for power law hardening:

$$\epsilon_{yy} = \frac{\sigma_{yy}}{E} + \left[\frac{\sigma_{yy}}{A}\right]^{1/n} \qquad (3)$$

E is Young's modulus, n is the strain hardening exponent and A is a material constant.

2. Equation (2) predicts unbounded stresses at the crack tip. Accordingly the stress field at $K = K_{ol}$ is calculated by offsetting the stress field by a small distance x_o:

$$\sigma_{yy}\,\epsilon_{yy} = \frac{K_{ol}^2}{\pi\,(1+n)\,E\,(x + x_o)} \qquad (4)$$

such that the stress σ_{yy} at $x = 0$ equals the tensile strength of the material.

3. The residual stress field induced by the overload σ_{res} is found by subtracting the stress field, $\Delta\sigma_{yy}$ due to unloading from K_{ol} to K_{min}, from the stress field at overload, $K = K_{ol}$. It is assumed that $\Delta\sigma_{yy}$ is given by:

$$\Delta\sigma_{yy}\,\Delta\epsilon_{yy} = \frac{(K_{ol} - K_{min})^2}{\pi\,(1+n)\,2E\,(x + x_o)} \qquad (5)$$

where $\Delta\epsilon_{yy}$ is related to $\Delta\sigma_{yy}$ via:

$$\frac{\Delta\epsilon_{yy}}{2} = \frac{\Delta\sigma_{yy}}{2E} + \left[\frac{\Delta\sigma_{yy}}{2A}\right]^{1/n} \qquad (6)$$

4. If crack advance into the overloaded region is simulated using a fine sawcut, while holding the load constant at the minimum load following the overload, P_{min}, then residual compressive stresses hold the crack shut. Hence it is argued that the stress field σ_{res} is the origin of K_{op} during crack growth through the overload plastic zone. Assume that the crack has advanced from the crack length at overload, a_{ol}, to a greater length, a. The K_{op} transient is assumed to take the form:

$$K_{op}(a) = K_{min} + \int_0^{a-a_{ol}} \frac{1}{\sqrt{2\pi}}\,\sigma_{res}(x)\,(a - a_{ol} - x)^{-\frac{1}{2}}\,dx \qquad (7)$$

where K_{min} is the minimum stress intensity of baseline fatigue loading and $(2\pi\,(a - a_{ol} - x))^{-\frac{1}{2}}$ is the Green's function for a point load a distance $(a - a_{ol} - x)$ from the tip of a semi-infinite crack in an infinite plate.

Equation (7) predicts that K_{op} increases with crack extension to a maximum value before decaying again to K_{min}. When K_{op} falls to the value associated with constant amplitude baseline loading the baseline value is used rather than equation (7).

Predictions of Model

The predictions of this model are compared in Fig.7 with the experimental results described previously for BS4360 50B steel. In order to examine the sensitivity of predicted crack growth rates with respect to a change of residual stress distribution, predictions are included for the case where the factor of π in equations (2) and (5) is replaced by $\pi/2$.

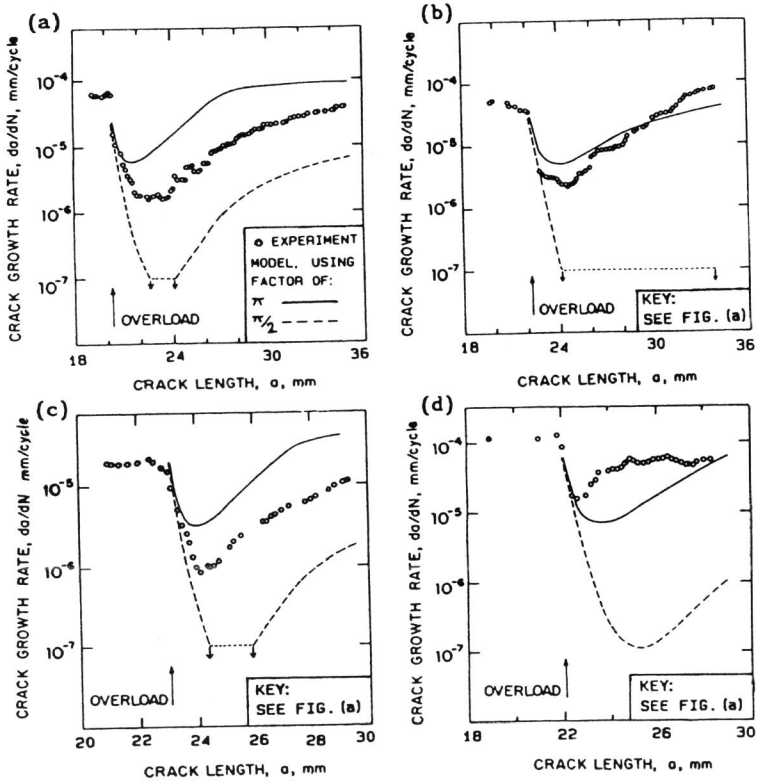

Fig. 7. Comparison of measured crack growth rates following an overload with those predicted by the simple model. In all cases, the overload cycle is of range twice the baseline loading. Baseline loading conditions for 3 mm thick specimens (plane stress):
(a) ΔK = 25 MPa$\sqrt{m}$, R = 0.05
(b) ΔK = 25 MPa$\sqrt{m}$, R = 0.3
(c) ΔK = 20 MPa$\sqrt{m}$, R = 0.05
and for 24 mm thick specimen (plane strain):
(d) ΔK = 25 MPa$\sqrt{m}$, R = 0.05.

It is apparent from Fig.7 that the predicted crack growth rate is very sensitive to the magnitude of the assumed residual stress distribution. Assuming that a factor of π is used in equations (2) and (5), the model is able to predict the retardation transient to within a factor of about 3 for the thin specimens (see Fig.7(a)-(c)). It is less accurate for the case of the 24 mm thick specimens (Fig.7(d)) where plane strain conditions prevail along most of the crack front. In this case, the predicted growth rates are up to 5 times slower than the measured growth rates and the model predicts retarded growth over a crack growth increment of about 3 times the observed value. This is consistent with the fact that the overload plastic zone size is much smaller under plane strain conditions than under plane stress conditions.

The model above is crude but has support on the following physical and theoretical grounds:

1. Allison (1979) has observed with the X-ray method that the residual stress field induced by an overload is not relaxed significantly by subsequent fatigue crack growth.
2. The model shows explicitly the manner in which residual stresses induced by the overload lead to increased closure values.
3. The assumed residual stress field σ_{res} resembles the Hutchinson-Rice-Rosengren field near the crack tip, and decays to the required elastic K-field far from the crack tip.
4. The sign of σ_{res} changes from compression to tension with increasing distance ahead of the crack tip from the overload position. Discontinuous closure is predicted in such a field.
5. The finite element results, Fig.4, suggest that retardation is not influenced by specimen geometry under plane stress conditions, and the simple model suffices. Under plane strain conditions, retardation is dependent upon specimen geometry via the T-stress, and a more complex retardation model is required.

CONCLUSIONS

Experimental and theoretical support is given for the hypothesis that plasticity-induced crack closure is one of the main causes of overload retardation, under both plane stress and plane strain conditions. Finite element results suggest that specimen geometry has a significant influence on crack growth delay when the specimen is sufficiently thick for plane strain conditions to prevail near the crack tip. A simple mechanics model has been developed which demonstrates the relationship between overload-induced residual stresses ahead of the crack tip and plasticity-induced crack closure.

ACKNOWLEDGEMENTS

The authors wish to thank Dr. J.C. Newman, Jr. for helpful discussions, and for financial support in the form of a NASA Research Grant.

REFERENCES

Allison, J.E. (1979). Measurement of crack tip stress distributions by X-ray diffraction. In: *Fracture Mechanics*, ASTM STP677 (C.W. Smith, Ed.), 550-562.

Fleck, N.A. (1982). The use of compliance and electrical resistance techniques to characterise fatigue crack closure. Cambridge University Engineering Department, Report CUED/C-MATS/TR89.

Fleck, N.A. (1984). An investigation of fatigue crack closure. Cambridge University Engineering Department, Report CUED/C-MATS/TR104.

Fleck, N.A. (1986). Finite element analysis of plasticity-induced crack closure under plane strain conditions. *Engng. Fract. Mech.*, 25(4), 441-449.

Fleck, N.A. and J.C. Newman Jr. (1988). Analysis of crack closure under plane strain conditions. In: *Mechanics of Fatigue Crack Closure*, ASTM STP982 (J.C. Newman and W. Elber, Ed.), 319-341.

Fleck, N.A., I.F.C. Smith, and R.A. Smith (1983). Closure behaviour of surface cracks. *Fatigue of Engng. Mats. and Structures*, 6(3), 225-239.

Fleck, N.A. and R.A. Smith (1982). Crack closure - is it just a surface phenomenon?. *Int. J. Fatigue*, July 1982, 157-160; correction in *Int. J. Fatigue*, Oct. 1982, p.243.

Larsson, S.G. and A.J. Carlsson (1973). Influence of non-singular stress terms and specimen geometry on small-scale yielding at crack tips in elastic-plastic materials. *J. Mech. Phys. Solids*, 21, 263-277.

Nagtegaal, J.C., D.M. Parks and J.R. Rice (1974). On numerically accurate finite element solutions in the fully plastic range. *Computer Methods in Applied Mechanics and Engineering*, 4, 153-177.

Newman, J.C., Jr. (1976). A finite element analysis of fatigue crack closure. In: *Mechanics of Crack Growth*, ASTM STP590, 281-301.

Rice, J.R. (1967). Stress due to a sharp notch in a work hardening elastic-plastic material loaded in longitudinal shear. *J. Appl. Mech.*, 34.2, 287-298.

Stouffer, D.C. and J.F. Williams (1979). A model for fatigue crack growth with a variable stress intensity factor. *Eng. Fract. Mech.*, 11, 525-536.